J Solid State Electrochem (2005) 9: 91–95
DOI 10.1007/s10008-004-0512-2

ORIGINAL PAPER

M. C. Santos · A. J. Terezo · V. C. Fernandes
E. C. Pereira · L. O. S. Bulhões

An EQCM investigation of charging RuO_2 thin films prepared by the polymeric precursor method

Received: 2 June 2003 / Accepted: 5 January 2004 / Published online: 16 July 2004

Abstract An electrochemical quartz crystal microbalance (EQCM) study of RuO_2 thin films, prepared by the sol-gel precursor method, is presented. The X-ray diffraction (XRD) analysis demonstrates that RuO_2 films were crystallized in the rutile phase and scanning electron microscopy investigations indicated the formation of a smooth surface. Cyclic voltammetry and EQCM studies were performed simultaneously in order to investigate the charging processes of the RuO_2 films in 0.1 M $HClO_4$. The voltammetric and mass versus potential responses present three well-defined regions associated with the RuO_2 redox couples. Based on these results and on the mass-charge relationships, the corresponding charging mechanisms are proposed. In the potential region governed by the Ru^{3+}/Ru^{4+} redox couple, the mass-charge relation can be associated with the double-injection of protons and electrons. The other regions correspond to water release and oxyhydroxide species formation during charging.

Keywords Electrochemical quartz crystal microbalance · RuO_2 · Pechini method · Electrochemical capacitors · Electrocatalysis

Introduction

Metal oxides, such as RuO_2, are important electrode materials in industrial electrolyses and energy storage devices. In particular, RuO_2 presents very high stability and low overpotentials for both the O_2 and Cl_2 evolution reactions [1] and it may also be advantageous for H_2 production. Although its overpotential for these reactions is higher than that of Pt, the use of RuO_2 is attractive because it is not very susceptible to contamination by metal deposition [2] or by adsorption of organic compounds [3]. Another important and emerging application of RuO_2 is in the field of electrochemical capacitors [4].

Although RuO_2 is intensively used in the applications cited above, much remains unknown concerning the specific electrochemical processes occurring at the RuO_2 electrolyte interface. Much of the controversy in past studies involved three complicating issues [5]: (1) the method of preparation that causes changes in the structure and composition, (2) the large number of stable Ru oxidation states and (3) slow background processes occurring in pores and at grain boundaries.

It is generally accepted that RuO_2 electrodes behave as "protonic condensers" [6] in the potential range between the hydrogen and oxygen evolution. In the course of a voltammetric experiment the RuO_2 surface is oxidized and reduced reversibly through a mechanism that involves proton exchange (double injection) with the solution [7, 8]:

$$RuO_x(OH)_y + \delta H^+ + \delta e^- \rightleftarrows RuO_{x-\delta}(OH)_{y+\delta} \quad (1)$$

The reaction described by Eq. 1 was also proposed to take place in anodically prepared hydrous oxides [9]. The difference lies in the fact that all the mass of the oxide is believed to be involved in Eq. 1 at the anodic oxide [10], while modifications only take place at the surface of crystallites of the thermally prepared oxide. Thus, in the latter case, the voltammetric charge is believed to be a measure of the number of sites that exchange protons with the solution [11], i.e., the electrochemically active surface area [12]. However, a precise correlation between the charge and the surface area is difficult because the exact nature of the surface reactions is unknown.

Recently, an electrochemical quartz crystal microbalance (EQCM) was used to study the electrochemical

M. C. Santos · A. J. Terezo · V. C. Fernandes · E. C. Pereira
L. O. S. Bulhões (✉)
Laboratório Interdisciplinar de Eletroquímica e Cerâmica,
Centro Multidisciplinar para o Desenvolvimento de Materiais Cerâmicos, Departamento de Química, Universidade Federal de São Carlos Rodovia Washington Luiz, CEP: 13565–905
São Carlos, SP, Brazil
E-mail: dlob@power.ufscar.br
Tel.: +55-16-261-5215
Fax: +55-16-260-8214

processes that occur in acidic media at ruthenium electrodeposited onto a gold substrate [13]. Complex voltammetric and mass variation behavior was observed when the potential was continuously cycled. Several types of non-stoichiometric surface reactions, which include the formation of various ruthenium oxyhydroxide species, were proposed.

In the present paper, the study of the electrochemical processes that occur during the charging of a sol-gel derived RuO_2 thin film (as opposed to the anodically deposited films presented in the literature and discussed in the last paragraph [13]) is presented. The investigations were performed using the techniques of cyclic voltammetry and piezoelectric microgravimetry (EQCM) simultaneously. The principal aim of the study was to correlate the mass and charge variations with mechanisms involved in the charge compensation during the oxidation and reduction of the ruthenium species formed in the RuO_2 thin films in acidic media.

Materials and methods

A single-compartment, three-electrode electrochemical cell made of Pyrex glass was used. The working electrode was a Pt/AT-cut quartz crystal of 9 MHz fundamental frequency. The RuO_2 film was painted over the Pt surface of the 0.2 cm^2 projected area. The RuO_2 films were prepared as described previously [14]. In the present investigation the precursor solution was composed of citric acid (CA), ethylene glycol (GE) and $RuCl_3.xH_2O$ (Ru) in the molar ratio of CA:GE:Ru equal to 1:4.65:0.33. This precursor solution was applied onto the Pt/quartz-crystal and thermally treated at 130 °C for 10 min, then at 250 °C for 20 min and finally at 400 °C for 30 min. The heating rate was 5 °C min^{-1} in a static air atmosphere.

The crystallinity of the films was examined by XRD, performed with the use of a Rigaku diffractometer model Dmax 2500PC with CuKα radiation ($\lambda = 1.5406$ Å). The morphology of the film was examined by scanning electron microscopy (SEM) using a ZEISS microscope, model DSM 940A.

The sensitivity factor for the EQCM was determined following the method previously described [15]. The value of the sensitivity factor ($\Delta f/\Delta m$) obtained was 6.25 ng Hz^{-1} cm^{-2}, which is higher than the fabrication standard, 5.5 ng Hz^{-1} cm^{-2} [16].

The electrochemical and piezoelectric microgravimetry experiments were performed using a potentiostat-galvanostat (EG&G PARC model 263A) linked to a quartz crystal analyzer (Seiko EG&G PARC model QCA917), both controlled by the EG&G PARC M270 software. All potentials are referred to the hydrogen electrode in the same solution (HESS). The voltammetric and mass versus potential curves were measured for 0.1 mol dm^{-3} $HClO_4$ in the potential range 0.4–1.4 V versus HESS ($P = 92$ kPa). Prior to the experiments, the solutions were de-aerated with N_2 for 30 min. A platinum foil was used as the auxiliary electrode.

Results and discussion

Figure 1 presents the XRD patterns of the RuO_2 film deposited onto Pt-quartz-crystal. The XRD pattern presents peaks corresponding to (110), (101), (211) and (220) crystal planes of RuO_2 in the rutile phase (PDF#40–1290). Metallic ruthenium is also observed at $2\theta = 44.4°$. The mean crystallite size, estimated by using the Scherer equation [17], was 12 nm using *hkl* (110). This result is in agreement with previous studies [14, 18].

The SEM images indicate that the surface of the RuO_2 film is smooth, compared to a typical "cracked-mud" film prepared for electrocatalytical and electrochemical capacitor purposes [19]. For the EQCM study, a cracked-mud morphology might cause difficulties in the interpretation of the mass responses as the active species can become trapped inside the porous structure. The smooth morphology was obtained by means of the controlled thermal treatment described in the experimental section.

Figure 2 shows the voltammetric curve (top), the mass response (middle) and charge variation vs. potential (bottom) for the RuO_2 coated electrode. The form of the voltammetric curves presented in Fig. 2 is characteristic of RuO_2 electrodes in acidic media [6, 14, 20]. The voltammetric curve is characterized by three pairs of broad anodic and cathodic peaks (labeled I, II and III) that correspond to redox couples. The presence of these transitions in the cyclic voltammogram is characteristic

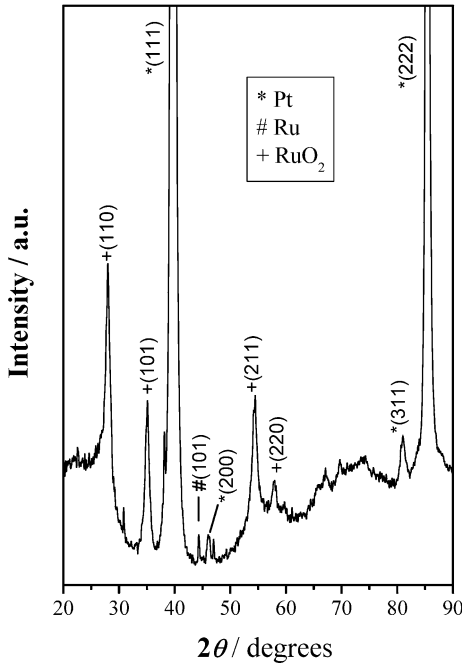

Fig. 1 X-ray diffraction patterns of the RuO_2 thin film calcinated at 400 °C

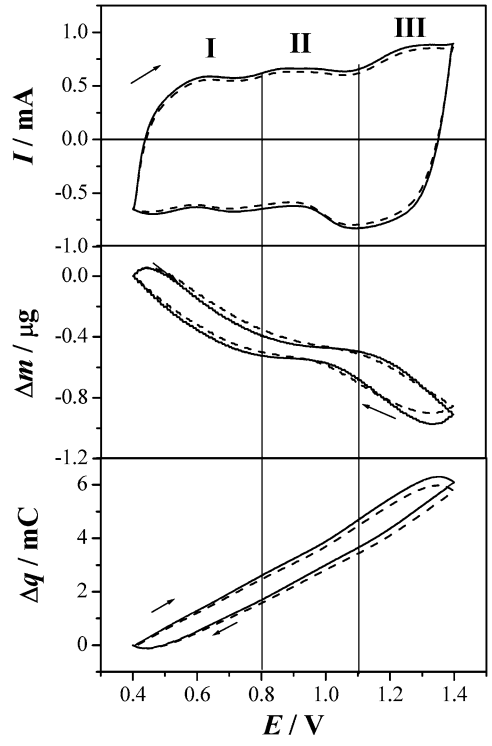

Fig. 2 Cyclic voltammogram, mass variations and charge vs. potential curves for RuO_2 in 0.1 M $HClO_4$ at 25 °C; potential sweep rate = 0.1 V s^{-1}, 1st cycle (*solid line*) and 40th cycle (*dashed line*)

of polycrystalline RuO_2 films and is widely described in literature [21, 22, 23]. Therefore, as proposed by Doblhofer et al. [24], it can be assumed that RuO_2 presents redox transitions from Ru^{2+} to Ru^{6+} in the potential range 0.4–1.4 V in acid solution. For this reason, the peaks observed in the voltammetric curve in Fig. 2 (top) can be associated with the following redox transitions: Ru^{2+}/Ru^{3+}, Ru^{3+}/Ru^{4+} and Ru^{4+}/Ru^{6+} with formal redox potentials of 0.56, 0.85 and 1.2 V, respectively.

The mass responses presented in Fig. 2 (middle) are somewhat more complex than the voltammetric responses and charge variations. During the anodic sweep from 0.4 to 1.4 V. the mass is observed to decrease by approximately 0.9 μg. For the reverse sweep from 1.4 to 0.4 V, approximately the same mass variation is obtained, but for a mass gain. This indicates that the processes involved are reversible. Furthermore, the 40th cycle (dotted line) is almost identical to the 1st, which indicates the stability of the redox processes.

Starting at 0.4 V and supposing that Ru^{2+} is the stable species at this potential, the first broad peak between 0.4 and 0.8 V (process I) corresponds to the transition Ru^{2+} to Ru^{3+}. For this process, an associated mass decrease of −0.4 μg was detected. After that, from 0.8 V to 1.15 V there is the transition Ru^{3+}/Ru^{4+} with a mass decrease of −0.09 μg. Peak III, in the range of 1.15 V to 1.4 V, corresponds to the transition Ru^{4+}/Ru^{6+} and this process results in a mass decrease of approximately −0.41 μg.

From the double-injection mechanism [7, 8], represented by equation Eq. 1, the oxidation of the RuO_2 film occurs with the simultaneous discharge of protons from the oxide matrix during the potential sweep between 0.4 and 1.4 V. However, the loss of one proton should correspond to a small mass variation. From the mass variations presented in Fig. 2, it seems that only the process between 0.8 and 1.15 V can be related to Eq. 1. It appears that other species are involved in the processes in regions I and III (Fig. 2 top).

The behavior of the mass variations as a function of the charge is depicted in Fig. 3, from which it is possible to propose the presence of three well-defined regions, I, II and III. The slopes are given in Table 1.

For region I, where the Ru^{2+} oxidation occurs, a molar mass of 32 g mol^{-1} was obtained. This value can be attributed to the loss of approximately two water molecules per RuO_2 site, as represented by the reaction:

$$RuO.xH_2O \rightarrow RuO(OH)(x - y)H_2O + 2H_2O + H^+ + 1e^- \quad (2)$$

Equation 2 is in agreement with the behavior observed for several types of non-stoichiometric oxides that contain various ruthenium oxyhydroxide species and water, as proposed for electrodeposited ruthenium in acidic medium during EQCM studies [13]. As two water molecules have been determined for each RuO_2 site, it is possible to affirm that the active sites of the surface are liberated when the ruthenium oxide is oxidized.

For region II (Fig. 3), a molar mass close to 1 g mol^{-1} was obtained (Table 1). After 0.8 V and up to 1.1 V (Δm = -0.09 μg) the Ru^{3+}/Ru^{4+} transition occurs with a slope close to 1 g mol^{-1}. This process can be described by Eq. 3:

$$RuO(OH)(x - y)H_2O \rightarrow RuO_2(x - y)(H_2O) + H^+ + 1e- \quad (3)$$

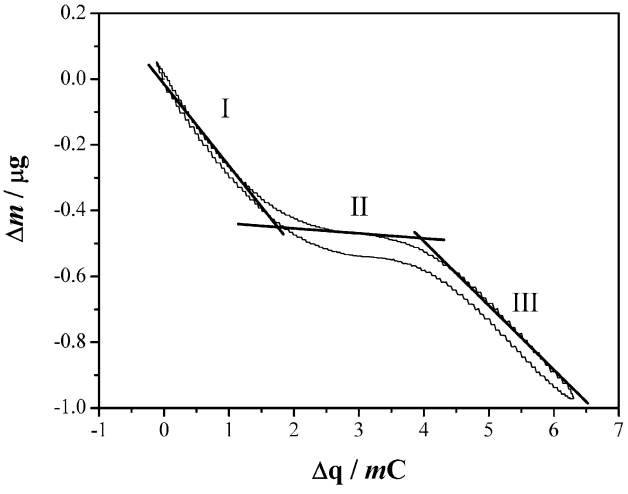

Fig. 3 Mass variation as a function of charge transferred in RuO_2 thin film electrodes

Table 1 Slopes and molar mass values for each potential region (obtained from Fig. 3)

Region	Slope	Molar mass
	g C^{-1}	g mol^{-1}
I	3.32×10^{-4}	32
II	1.00×10^{-5}	1
III	1.76×10^{-4}	17

This reaction, similar to Eq. 2, involves proton exchange with the solution [7, 8] and this explains the high charge density variation with a small change in the mass values between 0.8 and 1.1 V, which is related to the H desorption.

After 1.1 V and up to 1.4 V, $\Delta m = 0.41$ μg, (Fig. 3, region III) there is the transition of Ru^{4+} to Ru^{6+} and a slope of 17 g mol^{-1}. This value is probably due to H_2O and OH^- ($M_{H2O} = 18$ g mol^{-1} and $M_{OH} = 17$ g mol^{-1}), as already described for region I. As there is a two-electron transfer during the Ru^{4+}/Ru^{6+} transition, two water or two OH^- molecules per ruthenium oxide site are obtained. The mechanism proposed for region III can be described by the solid-state reaction:

$$RuO_2(x - y)H_2O \rightarrow RuO_3 + zOH^- + (z + 2)H^+ + 2e^- \quad (4)$$

where $z = 2$, and probably we have $RuO_2.3\ H_2O$. Considering the molar mass $(2M_{OH^-} + 4M_{H^+}/2 = 19$ g $mol^{-1})$, a value close to that found experimentally (17 g mol^{-1}) is obtained. As it is difficult to measure the hydrogen mass (due to its small molar mass), the experimentally obtained molar mass is that of OH^-.

The mechanism of the Ru^{6+} species formation in acidic medium has not been described in the literature yet. However, the use of potential modulated reflectance spectroscopy (PMRS) led to the proposal of the formation of RuO_4^{2-} species in alkaline solutions [25].

In the negative potential sweep from 1.4 V to 0.4 V the reduction of the oxide film, which was produced during the positive potential sweep, occurs. As a consequence the initial mass value is attained.

Another useful graphical representation to aid the interpretation of the response of the system is $d(\Delta m)/d\ t$ versus potential. Using Faraday's law $d(\Delta m)/d\ t$ is linearly related to the current by:

$$\frac{d(\Delta m)}{dt} = \frac{M}{nF} i \quad (5)$$

where Δm is the mass variation, M is the molar mass, n is the number of electrons transferred, Δq is the charge variation and i is the current. Considering that, during the oxidation or desorption, a mass loss occurs and during the electroreduction the process is associated with adsorption or ionic incorporation that leads to a mass increase, Eq. 5 can be altered to:

$$-\frac{d(\Delta m)}{dt} = \frac{M}{nF} i \quad (6)$$

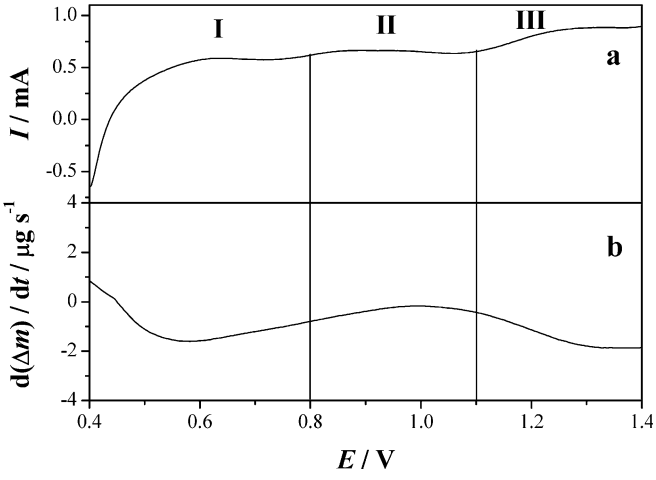

Fig. 4a, b Voltammetric (**a**) and $d(\Delta m)/d\ t$ (**b**) vs. potential curves for the anodic transient part of the cyclic voltammogram presented in Fig. 2

From Eq. 6 the current is linearly related to $d(\Delta m)/d\ t$ by the constant (M/nF). Thus, the form of $d(\Delta m)/d\ t$ versus potential should be the same as the voltammetric response for the same system.

Figure 4 shows the voltammetric and $d(\Delta m)/d\ t$ profile obtained from the curve presented in Fig. 2b. It can be observed that the processes in regions I and III exhibit a similar shape. In these regions, the $d(\Delta m)/d\ t$ plot is a mirror image of the anodic current in the voltammogram, as predicted by Eq. 6. In region II, the $(d(\Delta m)/d\ t)$ profile does not match the anodic current behavior. As a first approximation, it has to be considered that the mass for a proton results in a small variation in the $d(\Delta m)/d\ t$ profile while the anodic current exhibits a broad peak in the region of the redox couple. In fact, the response in this region can be attributed to a mass variation for proton "insertion/de-insertion", produced by the double-injection mechanism.

The reversibility of the system was investigated by cyclic voltammetry and mass variation experiments, using two potential scan rates: 0.05 and 0.02 V s^{-1} (see Fig. 2 for the response at 0.1 V s^{-1}). The combined results for both potential scan rates are shown in Fig 5a, b. From these results one can observe that the mass and charge values are little higher for 0.02 V s^{-1} than for 0.05 V s^{-1} which is related to a small increase in the time available for the processes to occur at the lower sweep rate (0.02 V s^{-1}).

In can be observed that the mass variation versus potential curve presents a smaller hysteresis at the sweep rate of 0.02 V s^{-1} (Fig. 5b). This effect is probably due to the longer time available for the electrochemical and mass transfer processes to occur at 0.02 V s^{-1} compared to 0.05 V s^{-1}.

Conclusions

In this paper, the voltammetric and EQCM investigations of the charging processes in RuO_2 thin films,

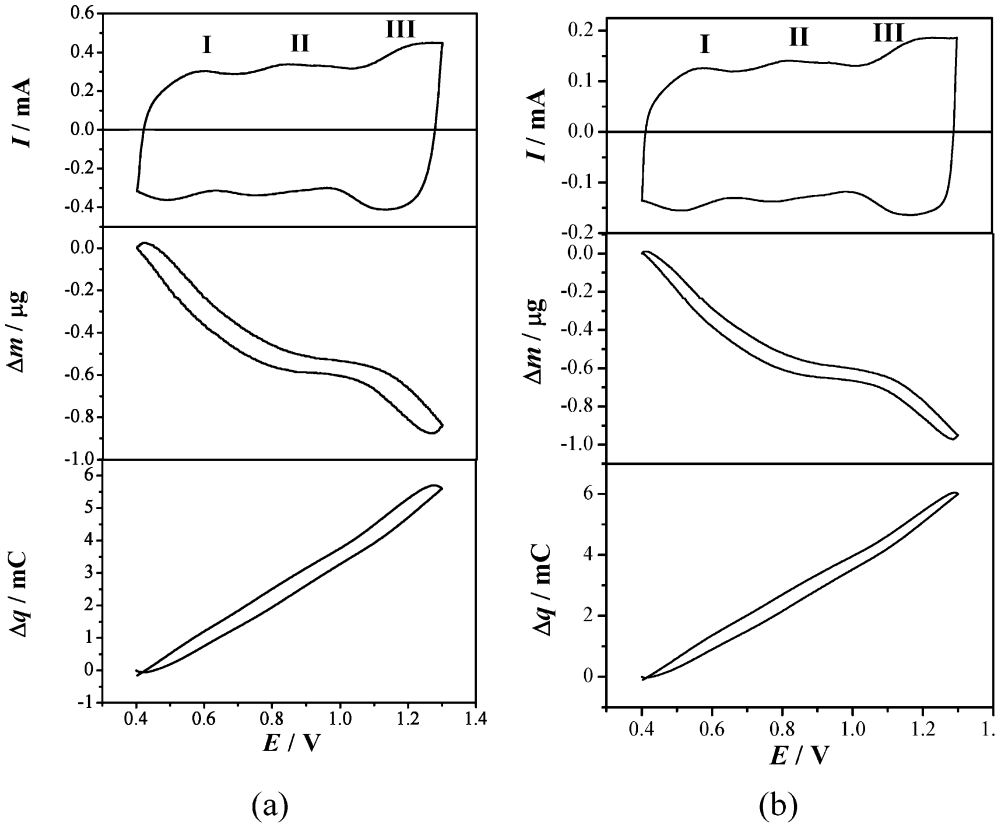

Fig. 5a, b Voltammetric, mass variation and charge vs. potential curves for the RuO_2 in 0.1 M $HClO_4$ at 25 °C; potential sweep rate: **a** 0.05, **b** 0.02 V s^{-1}

obtained by a modified sol-gel route, have been described for the first time. It was observed that the RuO_2 film is stable in the investigated potential region (0.4 and 1.4 V versus HESS) and presents greater reversibility at lower sweep rates. The RuO_2 oxidation/reduction mechanism was ascribed to different types of non-stoichiometric surface reactions, which include ruthenium oxyhydroxide species formation, water discharge and also proton exchange with the solution. EQCM experiments coupled with cyclic voltammetry proved to be very useful to obtain information concerning the mechanism of RuO_2 thin film oxidation and reduction in acidic medium. The results presented show that the proton step occurs only in the potential region associated with the Ru^{3+}/Ru^{4+} transition.

Acknowledgements The authors thank the Brazilian research funding institutions, CNPq and FAPESP.

References

1. Ardizzoni S, Trasatti S (1996) Adv Colloid Interface Sci 64:173
2. Kotz ER, Stucki S (1997) J Appl Electrochem 17:1190
3. Galizzioli D, Tantardini F, Trasatti, S (1975) J Appl Electrochem 5:203
4. Conway, B E (1999) Electrochemical supercapacitors. Kluwer, New York
5. Lister T E, Chu Y, Cullen W, You H, Yonco R M, Mitchell J F, Nagy Z (2002) J Electroanal Chem 524:201
6. Ardizzone S, Fregonara G, Trasatti S (1990) Electrochim Acta 35:263
7. Trasatti S, Buzzanca G (1971) J Electroanal Chem 29:1
8. Dobholfer K, Metikos M, Ogumi Z, Gerisher H, (1978) Ber Bunsenges Phys Chem 82:11
9. Michell D, Rand DAJ, Woods R (1978) J Electroanal Chem, 89:11
10. Burke, LD, Sullivan E JM (1989) J Electroanal Chem 117:155
11. Lodi G, Sivieri E, De Battisti A, Trasatti S (1978) J Appl Electrochem 8:135
12. Burke LD, Murphy OJ (1979) J Electroanal Chem 96:19
13. Vucovic M, Cukman D (1999) J Electroanal Chem 474:167
14. Terezo AJ, Pereira EC (2002) Mater Lett 53:339
15. Santos MC, Miwa DW, Machado SAS (2000) Electrochem Commun 2:692
16. Sauerbrey G (1959) Z Phys 155:206
17. Cullity BD (1967) Elements of X-ray diffaction, 3rd edn. Addison-Wesley, Massachusetts
18. Trasatti S (1991) Electrochim Acta 36:225
19. Conway BE, Birss V, Wojtowicz J (1997) J Power Sources 66:1
20. Trasatti S, Lodi G (1980) Properties of conductive transition metal oxides with rutile-type structure. In: Trasatti S (ed). Electrodes of conductive metallic oxides, part A. Elsevier, New York, p 334
21. Mattos-Costa FI, de Lima Neto P, Machado SAS, Avaca LA (1998) Electrochim Acta 44:1515
22. Wen TC, Hu CC (1992) J Electrochem Soc 139:2158
23. Angelinetta C, Trasatti S, Atanasoska Lj D, Atanasoski R T (1986) J Electroanal Chem, 214:535
24. Doblhofer K, Metikos M, Ogomi Z, Gerisher H (1978) Ber Bunsenges Phys Chem 82:85
25. Walker RC, Bailes M, Peter LM (1998) Electrochim Acta 44:1289